applied optics

Backscanning step and stare imaging system with high frame rate and wide coverage

CHONGSHANG SUN,[1,2,3,*] YALIN DING,[1,3] DEJIANG WANG,[1,3] AND DAPENG TIAN[1,3]

[1]Key Laboratory of Airborne Optical Imaging and Measurement, Changchun Institute of Optics, Fine Mechanics and Physics, Chinese Academy of Sciences, Changchun, Jilin 130033, China
[2]University of Chinese Academy of Sciences, Beijing 100049, China
[3]Changchun Institute of Optics, Fine Mechanics and Physics, Chinese Academy of Sciences, Changchun, Jilin 130033, China
*Corresponding author: sun2007cn@163.com

Received 12 February 2015; revised 28 April 2015; accepted 29 April 2015; posted 29 April 2015 (Doc. ID 234252); published 21 May 2015

Step and stare imaging with staring arrays has become the main approach to realizing wide area coverage and high resolution imagery of potential targets. In this paper, a backscanning step and stare imaging system is described. Compared with traditional step and stare imaging systems, this system features a much higher frame rate by using a small-sized array. In order to meet the staring requirements, a fast steering mirror is employed to provide backscan motion to compensate for the image motion caused by the continuously scanning of the gimbal platform. According to the working principle, the control system is designed to step/stare the line of sight at a high frame rate with a high accuracy. Then a proof-of-concept backscanning step and stare imaging system is established with a CMOS camera. Finally, the modulation transfer function of the imaging system is measured by the slanted-edge method, and a quantitative analysis is made to evaluate the performance of image motion compensation. Experimental results confirm that both high frame rate and image quality improvement can be achieved by adopting this method.

OCIS codes: (110.0110) Imaging systems; (110.4100) Modulation transfer function; (280.0280) Remote sensing and sensors.

http://dx.doi.org/10.1364/AO.54.004960

1. INTRODUCTION

Wide area coverage and high-resolution imagery remains one of the highest requirements for intelligence, surveillance, and reconnaissance systems. Current electro-optical and infrared sensors offer high-resolution imaging at the cost of a small field of view (FOV), which is the limiting factor on the utility of the imaging system. High-resolution images of wide areas are most commonly acquired by scanning a high-resolution camera. Previous imaging systems, such as second-generation infrared search and track (IRST) systems, employ line detectors with time delay and integration capability to improve signal-to-noise ratio (SNR) at the cost of a long exposure time [1]. However, limited by line detectors, it is impossible for scanning IRST systems to stop at any desired position to concentrate on a small area of interest [2]. Another resolution is step and stare imaging with small-sized staring arrays, in which wide area coverage imagery is formed by stitching together separate images [3]. But in traditional step and stare imaging systems, the settling time required to perform a cyclic start/stop motion with the massive gimbal is too long, and the step rate is limited to several frames per second [4,5]. To increase the frame rate of the imaging system, fast steering mirror (FSM) is employed to perform the backscan function that cancels the gimbal's continuous scan motion during exposure [6]. In backscanning step and stare imaging systems, the scanning motion of the gimbal is rapid, continuous, and smooth, thus reducing frame-to-frame settling time. Compared with conventional mass-stabilized and mirror-stabilized systems, the FSM, which is usually actuated by the piezoelectric ceramic or voice coil motor, has a higher bandwidth and higher precision at the cost of a smaller angular range and a smaller size [7–9]. FSMs have been applied in many optical systems to improve beam control performance, ranging from free space communication to adaptive optical systems and astronomical telescopes [10–12].

Despite the advantages of backscanning, such as high frame rate and image quality improvement, having been discussed [13], there still exist questions to be solved, for instance, how to put the concept into practice and how to verify the concept with imaging experiments. Since the image quality of the backscanning step and stare imaging system is determined by the performance of the image motion compensation system, an objective criterion needs to be developed to evaluate the performance of the image motion compensation system. Currently, whether the performance of the image motion compensation system meets the imaging requirements is usually judged by human eyes [14], and the result varies from person to person,

which is not reliable. In this paper, the modulation transfer function (MTF) is introduced as a quantitative criterion to assess the performance of the image motion compensation system.

Our research objective is to introduce MTF to analyze the experimental results of the backscanning step and stare imaging system. In this article, the backscanning step and stare imaging system is described in Section 2, including system components, operating principle, and control system design. The slanted-edge method and modeling of the scanning image motion in the MTF manner are briefly discussed in Section 3. In Section 4, a proof-of-concept backscanning imaging system is established and a series of experiments is conducted to measure the MTF by using the slanted-edge method.

2. BACKSCANNING STEP AND STARE IMAGING SYSTEM

A. System Components and Operating Principle

When the aircraft flies across the target area, the airborne imaging system sweeps out successive and overlapping images that are then stitched together to form a gapless image of the target zone, as illustrated in Fig. 1. The traditional step and stare imaging system moves the gimbal to a field of view, stops the gimbal to stare at the target area during exposure, then moves the gimbal to the starting position and repeats the same movement to the next field of view [4]. Since the gimbal is always large and massive, it is difficult to accelerate and position the gimbal repeatedly with high accuracy. Furthermore, the settling time required to cyclically stop and restart the whole gimbal is too long, so the frame rate will not be high.

Figure 2 depicts the basic components of the backscanning step/stare imaging system that avoid the above problems and disadvantages in traditional systems. An afocal optical system is mounted on a gimbal, which rotates at a constant speed and isolates the imaging system from undesirable aircraft movement. Typically, the gimbal provides two or more axes of rotation, but only one axis is illustrated in order to simplify

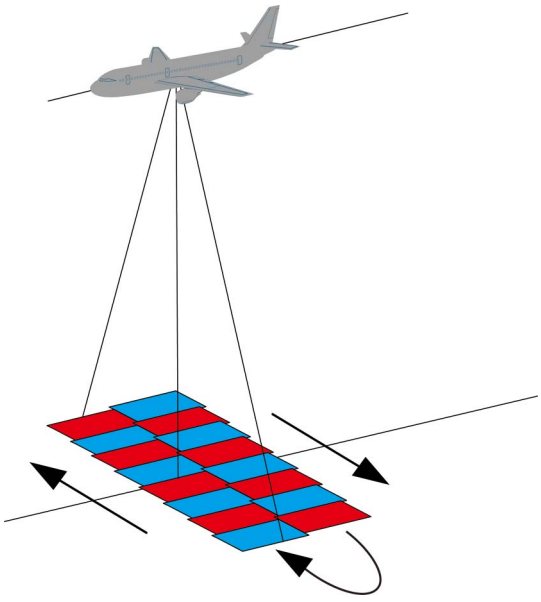

Fig. 1. Step and stare concept.

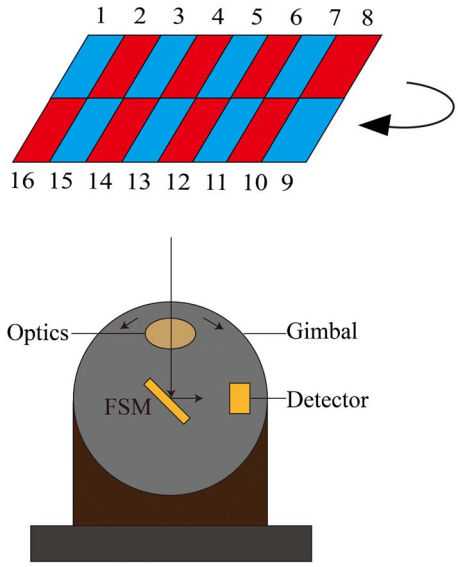

Fig. 2. Physical layout of the backscanning step and stare imaging system.

the statement of the imaging process. A FSM, which is used as an image motion compensation (IMC) mirror, reflects the image area into the staring focal plane array.

As the gimbal continuously rotates at a constant rate, the field of view across a target image area is swept by the afocal optics. During integration time, the FSM rotates in the opposite direction to the gimbal motion to keep the line of sight stationary and stabilized. Once an image is integrated, the FSM is accelerated in the same direction as the gimbal motion to return to its starting position so that the next field of view can be taken in the same way. In order to catch up with the rotation of the gimbal and hold the LOS of the next image frame, the speed of the FSM is much higher than that of the gimbal. When one scan bar (from image 1 to image 8) is terminated, the gimbal directs the sensor LOS to image area 9 and scans the subsequent scan bar (from image 9 to image 16) in the opposite direction, the sequence of image acquisition is described in Fig. 2. Figure 3 illustrates the timing/position relationships among the gimbal platform, the backscanning mirror, and the LOS of the imaging system. The image acquisition of the detector is controlled by trigger signals originating from the servo control system, and integration time is several milliseconds, which is also shown in Fig. 3.

In the backscanning step and stare imaging system the gimbal continuously rotates at a constant speed to step the LOS of the sensor and the backscan operation of the FSM compensates for the image motion during exposure to meet the staring requirements. In this way, only the small FSM is required to be repeatedly accelerated and positioned, thus reducing frame-to-frame settling time. Moreover, the control precision of the FSM is usually several microradians or less, which is much higher than the gimbal. In a word, this design can not only highly improve step and stare performance, but also make full use of the high frame rate of the small-sized array. Figure 4 describes another mechanical design of the backscanning step and stare imaging system. A gimbaled mirror is placed in the

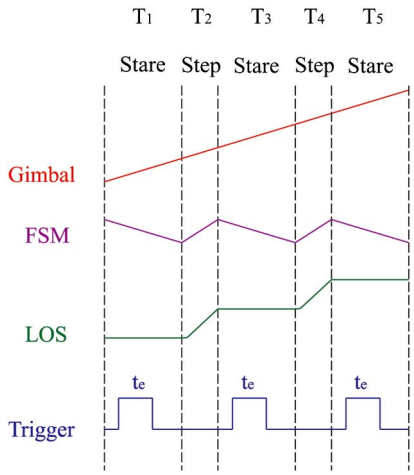

Fig. 3. Timing/position relationships among the gimbal, the FSM, and the LOS, timing diagram of the exposure trigger signal during imaging.

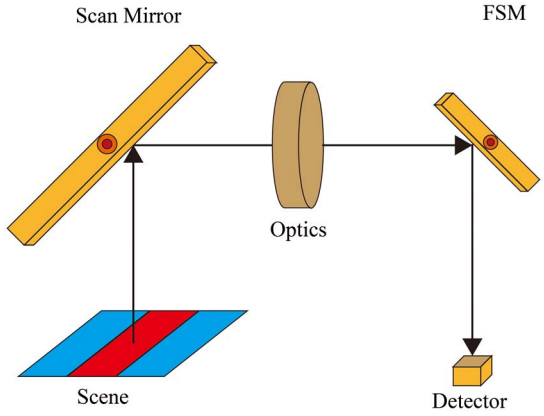

Fig. 4. Backscanning step and stare imaging system in which a scan mirror is used instead of the gimbal.

optical path to scan the target area at a constant rate and the FSM performs the backscan function to remove the image motion during the exposure time [7].

B. Control System Design

The main challenge for the step and stare imaging system is the design of the control system [6]. The control system must step/stare the LOS at a high frame rate with a high precision. The bandwidth of the control system determines the imaging system's frame rate, while the control accuracy affects the imaging performance. As illustrated in Fig. 5, the primary servo loops encompass the gimbal rate stabilization loop and the IMC loop. The gimbal stabilization loop ensures that the gimbal rotates in response to the input command with gyro feedback. What is more, the other role of the stabilization loop is to isolate the imaging system from undesirable disturbance. The input of the IMC loop is the measured gimbal rate error multiplied by the IMC mirror scale factor, which is expressed as $aM/2$. M is the magnification of the optical system and a is the scale factor adjustment term. The mirror scale factor adjustment term must be calibrated in flight because of undesirable disturbance introduced by the change of the operating environment [5]. For instance, temperature variation and bearing friction may lead to the speed mismatch between the gimbal and the FSM.

3. MTF AND SLANTED-EDGE METHOD

A. Slanted-Edge Method

The MTF, which describes how spatial frequencies are modified by imaging systems, is widely used to evaluate the performance of imaging systems. Many methods have been established and used to measure MTF, such as the sine target method and knife edge method [15], but they either need a long measurement time, or lack measurement precision. The slanted-edge technique provides a fast MTF measurement method based on only one image, which is effective and simple [16,17]. Because of these advantages, the slanted-edge method has been used to measure MTF on orbit [18,19], and modified methods have been proposed to improve the measuring accuracy [20,21].

Compared with the knife edge method, the edge is slightly slanted in order to increase the sampling frequency and avoid the aliasing effect. A rectangular region of interest (ROI) is selected in the image of the knife edge target. By using the super-resolution technique, the data in the ROI are projected along the direction of the edge to generate a 1D edge spread function.

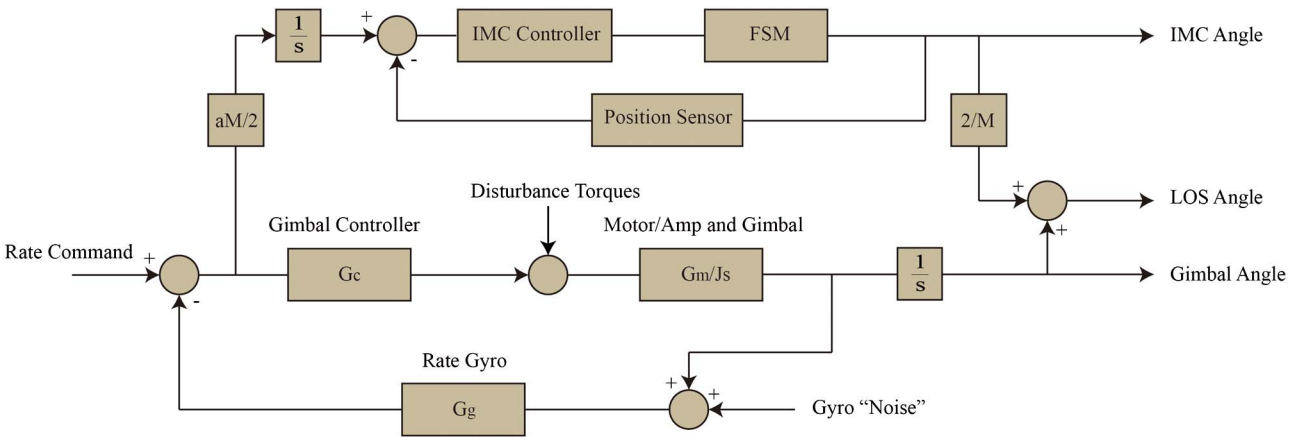

Fig. 5. Single-axis LOS control system block diagram for a backscanning step and stare imaging system.

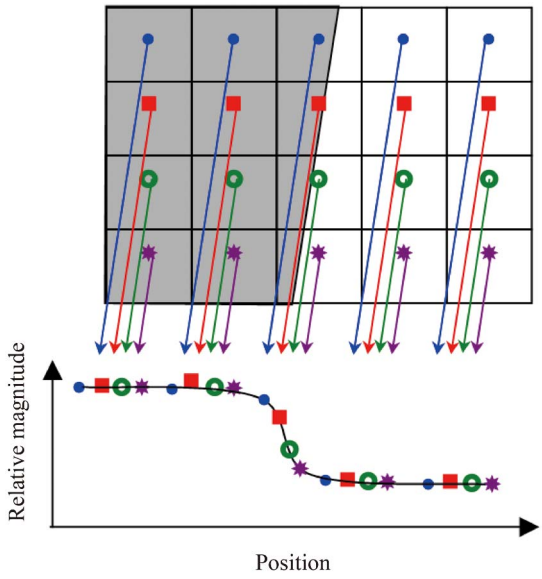

Fig. 6. Projection of the data along the edge.

The process is illustrated in Fig. 6. Mathematical methods are used to fit the edge spread function to subpixel accuracy. The line spread function (LSF) is obtained by calculating the first derivative of the supersampled and fitted ESF. MTF is a 1D Fourier transform of the LSF, which is normalized at zero frequency. The procedure of calculating the MTF from ESF is shown in Fig. 7.

B. Modeling of MTF Degradation Caused by Scanning Image motion

For high-resolution imaging systems, the degradation of the image quality due to image motion is always described by the MTF [22]. In the backscanning step and stare imaging system, scan motion is completely compensated for by the FSM only if

$$\omega_g = \frac{2}{M}\omega_m, \tag{1}$$

where M represents the magnification of the optical system, and ω_g and ω_m are the angular speed of the gimbal and the FSM, respectively. Speed mismatch between the gimbal and the FSM leads to MTF degradation, which can be expressed by a sinc function,

$$\mathrm{MTF}_{\mathrm{motion}} = \mathrm{sinc}\left[\left(\omega_g - \frac{2}{M}\omega_m\right) f t_e \xi\right], \tag{2}$$

where t_e is the exposure time, f is the focal length of the optical system, and ξ represents the spatial frequency. The total MTF is the MTF of the imaging system multiplied by $\mathrm{MTF}_{\mathrm{motion}}$,

$$\mathrm{MTF}_{\mathrm{total}} = \mathrm{MTF}_{\mathrm{system}} \times \mathrm{MTF}_{\mathrm{motion}}. \tag{3}$$

$\mathrm{MTF}_{\mathrm{system}}$ can be measured by the slanted-edge method when the gimbal and the FSM are both still, and $\mathrm{MTF}_{\mathrm{total}}$ can be measured when the imaging system works in step and stare mode. By comparing $\mathrm{MTF}_{\mathrm{total}}$ with $\mathrm{MTF}_{\mathrm{system}}$, we can make an quantitative assessment of the step and stare imaging system's performance.

4. EXPERIMENTS AND RESULTS

A. Experimental Setup

As illustrated in Fig. 8, an integrating sphere is used to provide uniform illumination for the bar target, and the light passes through the collimator before coming into the step and stare imaging system. The proof-of-concept backscanning step and stare imaging system is shown in Fig. 9. In the imaging system, the platform where FSM, the optical system, and the CMOS sensor are mounted rotates at a constant speed. Both the platform and the FSM are controlled by a DSP28335, and the 2 K × 2 K CMOS camera works in external trigger mode. Once the LOS is stabilized, the camera starts exposure that is controlled by the image acquisition trigger signal originating from DSP28335.

Since the image motion compensation is accomplished by the FSM, the performance of the FSM must be evaluated when designing the control system. In our experiment, the angular travel of the mirror is ±1°, the bandwidth of the FSM control system is more than 100 Hz, and the position error is less than 6 μrad root-mean-square (RMS). However, the performance of the image motion compensation is also affected by other factors in the imaging system, such as the focal length, the pixel size, and the exposure time. The focal length of the imaging system is 200 mm, the pixel size of the CMOS sensor is 5.5 μm, and the exposure time is 5 ms. Considering the performance of the image motion compensation system, the gimbal platform rotates at a speed of 8 degree/second, and the frame rate is set up to 50 Hz.

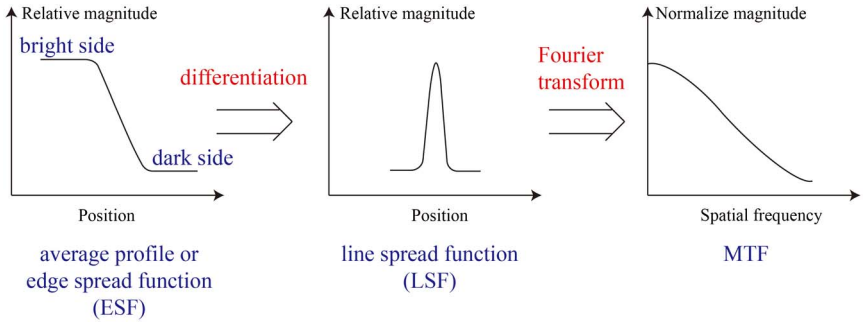

Fig. 7. Calculation of the MTF from ESF.

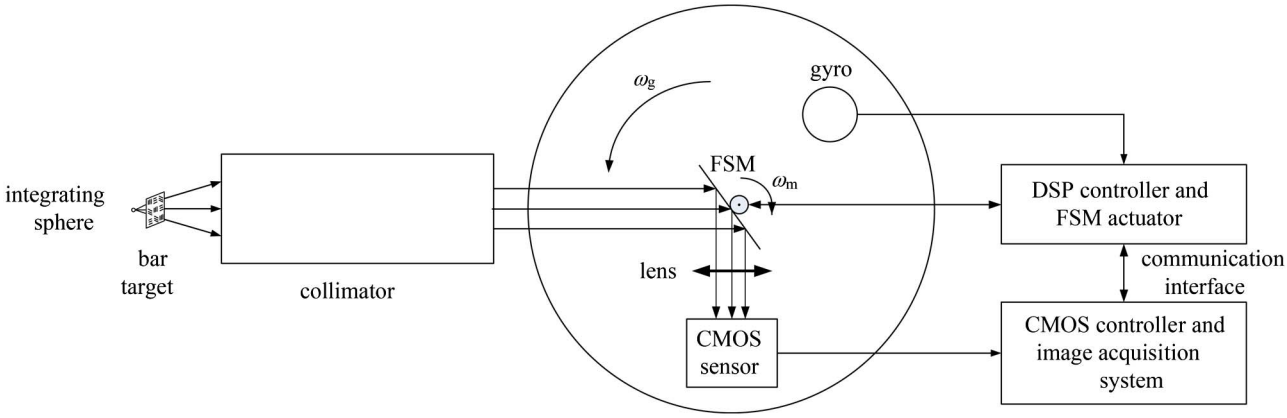

Fig. 8. Sketch of the experimental setup.

B. Results and Analysis

First, the resolution target is used to evaluate the image motion compensation performance of the FSM, as is shown in Fig. 10. According to general principles of geometrical optics, the size of the bar target pattern and the size of the image satisfy the following relationship [14]:

$$\frac{f_{\text{Collimator}}}{f_{\text{Camera}}} = \frac{W_{\text{Target}}}{W_{\text{Image}}}, \tag{4}$$

where $f_{\text{Collimator}}$ and f_{Camera} stand for the focal length of the collimator and camera, respectively, W_{Target} is the width of a bar, and W_{Image} is the width of the bar image. For a fixed focal length of the collimator, the pixel size becomes the limiting factor when choosing the resolution target. If higher spatial frequencies are required, a smaller target should be selected. In our experiment, the focal length of the collimator and the CMOS camera are 1500 and 200 mm, respectively. Note that the Nyquist frequency determined by the pixel pitch is

$$f_N = \frac{1}{2p}, \tag{5}$$

where p represents the pixel pitch of the CCD or CMOS sensor, and with units of cycles/mm. For our experiment, the pixel pitch of the CMOS camera is 5.5 μm, and the Nyquist frequency equals 91 cycles/mm. In Fig. 10(b) the spatial frequency of the smallest target we can resolve is 12 cycles/mm, which is close to the Nyquist frequency, according to Eq. (4). The results prove that the FSM can effectively compensate for the image motion caused by scanning.

Figure 11 shows images of an outdoor scene captured by the imaging system. From Figs. 11(a) and 11(b), it can be seen that the image quality is greatly improved by using the FSM to remove the image motion. In Fig. 11(b), the Chinese characters on the near building can be resolved, and the chimneys in the distance can be seen clearly.

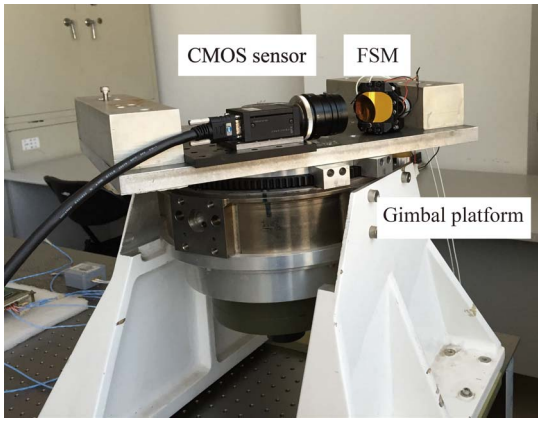

Fig. 9. Proof-of-concept backscanning step and stare imaging system.

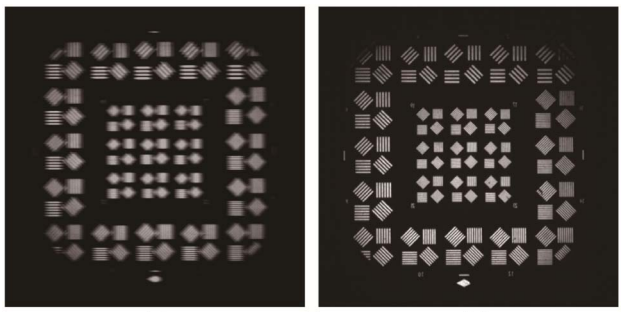

Fig. 10. Images of resolution target (a) without image motion compensation, (b) with image motion compensation by the FSM.

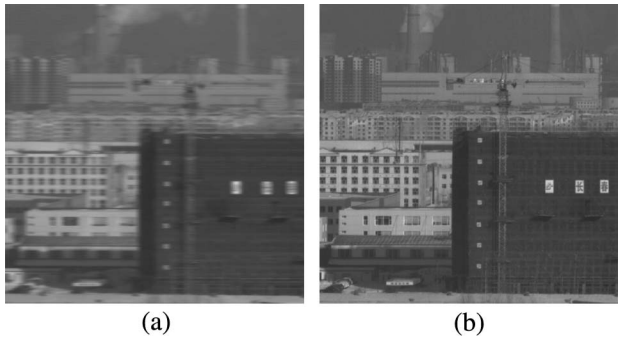

Fig. 11. Images of outdoor scene (a) without image motion compensation, (b) with image motion compensation by the FSM.

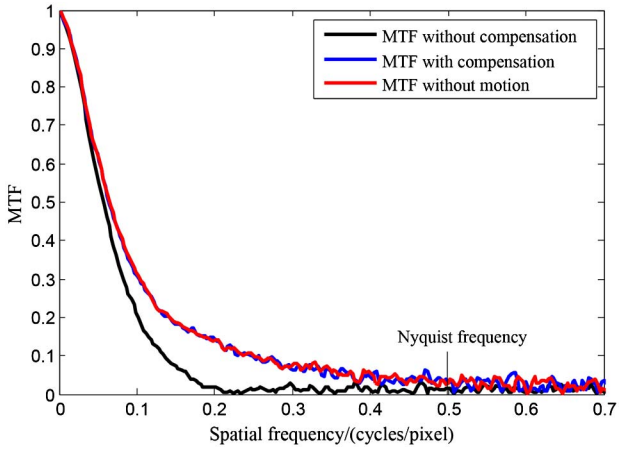

Fig. 12. MTF measured by the slanted-edge method.

However, the methods described above cannot provide a quantitative analysis, which is always needed to tell the designers how much the performance of the image motion compensation system should be improved in engineering. Since image motion leads to MTF degradation, we introduce the MTF to evaluate the performance of the image motion compensation system. By using the slanted-edge method, MTF_{system} is measured when the whole system remains still, which is shown by the red line in Fig. 12. In Fig. 12, the black line represents the MTF without image motion compensation, which reflects the image quality degradation due to image motion. The blue line is obtained when the FSM is used to cancel image motion, which is nearly equal to the red line below the Nyquist frequency. Considering that the MTF measured by the slanted-edge method beyond the Nyquist frequency is not reliable, the results confirm that the backscan operation of the FSM can meet the staring requirements during exposure.

5. CONCLUSIONS

In this paper, we have developed a backscanning step and stare imaging system with a small-sized staring array. In the imaging system, the FSM provides a backscan operation against the continuously scanning of the gimbal platform where the afocal optical assembly and the FSM are mounted. Compared with the traditional imaging systems, the main advantage of the imaging system is that the frame rate is much higher without requiring the massive gimbal to be repeatedly stopped and restarted. The frame rate of the established proof-of-concept imaging system is 50 Hz, which increases the size of the area scanned in a given time. Since the image motion compensation of the FSM directly affects the image quality, the MTF is introduced as an objective performance criterion of the image motion compensation. The quantitative analysis of the MTF by the slanted-edge method proves that the image motion compensation of the FSM can meet the staring requirements. In short, the backscanning step and stare imaging system can be used for wide area surveillance and high frame rate tracking. We hope this study will be useful in the design of imaging systems as well as in the performance evaluation of image motion compensation.

National Natural Science Foundation of China (NSFC) (61304032, 61308099).

REFERENCES

1. G. Barani, M. Olivieri, C. Luison, A. Rossi, M. Diani, and N. Acito, "Development of a panoramic third generation IRST: initial study and experimental work," Proc. SPIE **8704**, 87040J (2013).
2. R. Venkateswarlu, M. H. Er, S. C. Tam, C. W. Chan, and L. C. Choo, "Design considerations of IRST system," Proc. SPIE **3061**, 591–602 (1997).
3. I. Greenfeld, Z. Yavin, and B. Uhl, "Airborne reconnaissance system," U.S. patent 7,136,726 (14 November 2006).
4. M. Amon and B. Stokes, "Stabilized step/stare scanning device," U.S. patent 5,663,825 (2 September 1997).
5. P. V. Messina, "System and method for remote image sensing and autocalibration," U.S. patent 5,672,866 (30 September 1997).
6. K. J. Held and B. H. Robinson, "TIER II plus airborne EO sensor LOS control and image geolocation," in *IEEE Aerospace Conference Proceedings* (IEEE, 1997), pp. 377–405.
7. J. M. Hilkert, "Inertially stabilized platform technology," IEEE Control Syst. Mag. **28**(1), 26–46 (2008).
8. J. L. Miller, S. Way, and B. Ellison, "Design challenges regarding high-definition electro-optic/infrared stabilized imaging systems," Opt. Eng. **52**, 061310 (2013).
9. H. L. Gutierrez, J. D. Gaines, and M. R. Newman, "Line-of-sight stabilization and back scanning using a fast steering mirror and blended rate sensors," in *Infotech@Aerospace 2011*, (American Institute of Aeronautics and Astronautics, 2011), pp. 1–8.
10. D. J. Kluk, "*An Advanced Fast Steering Mirror for Optical Communication*," (Massachusetts Institute of Technology, 2007).
11. C. E. Max, S. S. Olivier, H. W. Friedman, J. An, K. Avicola, B. V. Beeman, H. D. Bissinger, J. M. Brase, G. V. Erbert, D. T. Gavel, K. Kanz, M. C. Liu, B. Macintosh, K. P. Neeb, J. Patience, and K. E. Waltjen, "Image improvement from a sodium-layer laser guide star adaptive optics system," Science **277**, 1649–1652 (1997).
12. M. Cho, A. Corredor, C. Dribusch, W. H. Park, M. Sheehan, M. Johns, S. Shectman, J. Kern, C. Hull, Y. S. Kim, and J. Bagnasco, "Performance prediction of the fast steering secondary mirror for the giant Magellan telescope," Proc. SPIE **8444**, 84424 (2012).
13. P. O. Nouguès, P. Baize, F. Roland, J. F. Olivier, and M. Renaudat, "Third-generation naval IRST using the step-and-stare architecture," Proc. SPIE **6940**, 69401B (2008).
14. D. Wang, T. Zhang, and H. Kuang, "Clocking smear analysis and reduction for multi phase TDI CCD in remote sensing system," Opt. Express **19**, 4868–4880 (2011).
15. M. Estribeau and P. Magnan, "Fast MTF measurement of CMOS imagers using ISO 12233 slanted-edge methodology," Proc. SPIE **5251**, 243–252 (2004).
16. P. D. Burns, "Slanted-edge MTF for digital camera and scanner analysis," in *Proceedings of PICS 2000* (Society for Imaging Science and Technology, 1998), pp. 135–138.
17. S. Najafi and K. Madanipour, "Measurement of the modulation transfer function of a charge-coupled device array by the combination of the self-imaging effect and slanted edge method," Appl. Opt. **52**, 4724–4727 (2013).
18. M. K. Rangaswamy, "Quickbird II: Two-Dimensional On-Orbit Modulation Transfer Function Analysis Using Convex Mirror Array," Master's thesis (South Dakota State University, 2003).
19. R. Ryan, B. Baldridge, R. A. Schowengerdt, T. Choi, D. L. Helder, and S. Blonski, "IKONOS spatial resolution and image interpretability characterization," Rem. Sensing Environ. **88**, 37–52 (2003).
20. T. Li, H. Feng, and Z. Xu, "A new analytical edge spread function fitting model for modulation transfer function measurement," Chin. Opt. Lett. **9**, 031101 (2011).
21. K. Masaoka, T. Yamashita, Y. Nishida, and M. Sugawara, "Modified slanted-edge method and multidirectional modulation transfer function estimation," Opt. Express **22**, 6040–6046 (2014).
22. R. D. Fiete, "Motion," in *Modeling the Imaging Chain of Digital Cameras* (SPIE 2010), pp. 99–108.